



Vietnam Academy of Science and Technology

National Institute for Materials Science of Japan

PROCEEDINGS

The 9th International Workshop on Advanced Materials Science and Nanotechnology

The 9th International Workshop on Advanced Materials Science and Nanotechnology



Ninh Binh City, Vietnam, November 7-11th, 2018

**The 9th International Workshop on
ADVANCED MATERIALS SCIENCE AND
NANOTECHNOLOGY**

**IWAMSN 2018
November 7 – 11th, 2018
Ninh Binh, Vietnam**

ORGANIZERS



Vietnam Academy of Science and Technology (VAST)

National Institute for Materials Science of Japan (NIMS)

SPONSORS

Vietnam Academy of Science and Technology (VAST)



Institute of Materials Science, VAST (IMS)



Institute of Physics, VAST (IOP)



**National Institute for Materials Science of Japan
(NIMS)**



Asian Pacific Center for Theoretical Physics (APCTP)



**National Foundation for Science and Technology
Development (NAFOSTED)**



**Editorial Board of Advances in Natural Sciences:
Nanoscience and Nanotechnology**



SISC Vietnam Instrumentation Joint Stock Company



ACETECH



RED STAR Vietnam



HORIBA Scientific



TABLE OF CONTENT

PART I

List of selected abstracts published in journal *Advances in Natural Sciences: Nanoscience and Nanotechnology*

		CODE	STATUS
1	Anomalies in one-dimensional electron transport: quantum point contacts and wires <i>Mukunda P Das and Frederick Green</i>	SPL-04	To be published
2	Quantitative measure of nitrogen vacancy related effects in SmN and EuN <i>Muhammad Azeem</i>	AMC-O08	Art. num. 015003, Issue 1, Vol. 10, 2019
3	Structural, optical and electrical properties of ribbon-like graphene oxide thin films <i>T. H. T. Aziz and M. M. Salleh</i>	MEP-O11	To be published
4	Synthesis of magnetic iron oxide/graphene oxide nanocomposites for removal of cadmium ions from water <i>Lu Thi Mong Thy, Thuong Nguyen Hoai, Tu Tran Hoang, Phong Mai Thanh, Nam Hoang Minh, Hieu Nguyen Huu</i>	NLE-P34	To be published
5	Doxycycline loaded Fe₃O₄ nanoparticles: preparation and evaluation on growth and survival of White Leg shrimp (<i>Litopenaeus vannamei</i>) <i>Phan Ke Son, Nguyen Hoai Nam, Vu Thi Tuyet Thuy, Do Hai Doan, Le Thi Thu Huong, Mac Nhu Binh, Dang Dinh Kim, Ha Phuong Thu</i>	NLE-P36	To be published
6	Preparation of doxycycline loaded Ag decorated TiO₂ nanoparticles for improving bacterial treatment effectiveness in White-leg shrimp (<i>Litopenaeus vannamei</i>) <i>Thi Tuyet Thuy Vu, Thi Kim Anh Le, Hoai Nam Nguyen, Ke Son Phan, Hai Doan Do, Thi Thu Huong Le, Nhu Binh Mac, Dinh Kim Dang, Phuong Thu Ha</i>	NLE-P37	To be published

	polypyrrole films synthesized by vapour-phase polymerization with regulating FeCl₃ oxidant concentration		
	<i>Hoang Thi Hien, Ho Truong Giang, Do Thi Anh Thu, Giang Hong Thai, Pham Quang Ngan, Bui Ha Trung, Bui Nguyet Nhung, Chu Van Tuan, Tran Trung, Nguyen Thanh Huy</i>		
13	Multiband and broadband absorber metamaterial creating by multi porous square layers structure	MEP-P10	90
	<i>Tran Manh Cuong, Nguyen Thuy Hien, Nguyen Thi Thuy, Pham Van Hai, Vu Dinh Lam</i>		
14	In-situ STM studies of ordered arrays of porphyrin molecules on bromide modified Cu(111) under electrochemical control	MEP-P13	95
	<i>Phi Hung Nguyen, Thi Mien Trung Huynh, Vien Vo, Van Hoang Cao, Klaus Wandelt and Thanh Hai Phan</i>		
15	Low temperature textured growth of 9-chloroanthracene films for electronics and photonics	MEP-P15	104
	<i>Sukhwinder Singh Brar, Harpreet Kaur, Dinesh Pathak</i>		
16	Crystal transformation of thermally annealed titanium dioxide nanotubes revealed by photoluminescence emission and Raman scattering vibration	MEP-P16	110
	<i>Nguyen Huu Tho, Vo Cao Minh, Luu Thi Lan Anh, Nguyen Xuan Sang</i>		
17	Impact of external factors on electromagnetic properties of metamaterial absorbers in THz region	MEP-P18	115
	<i>Nguyen Minh Nguyet, Pham The Linh, Dang Hong Luu, Bui Xuan Khuyen, Tran Manh Cuong, Le Duc Tuyen, Vu Dinh Lam</i>		
18	Effect of size and shape on characteristics of Fe₃O₄ nanoparticles	MEP-P19	121
	<i>Vuong Thi Kim Oanh, Do Hai Doan, Nguyen Xuan Truong, Nguyen Xuan Ca, Le The Tam, Le Trong Lu, Tran Dai Lam</i>		
19	Anisotropic optical characterizations of artificial opal photonic crystal	MEP-P26	128
	<i>Le Duc Tuyen, Tong Ba Tuan, Du Thi Xuan Thao, Tran Thu Huong, Le Quoc Minh, Vu Dinh Lam, and Chia Chen Hsu</i>		
20	Influence of Cr-addition on magnetic properties and magnetocaloric effect of Fe-Cr-Gd-Zr-B rapidly quenched alloys	MEP-P28	134

CODE: MEP-P19

Effect of size and shape on characteristics of Fe₃O₄ nanoparticles

Vuong Thi Kim Oanh^{1,*}, Do Hai Doan¹, Nguyen Xuan Truong¹, Nguyen Xuan Ca², Le The Tam³, Le Trong Lu⁴, and Tran Dai Lam⁴

¹Institute of Materials Science, Vietnam Academy of Science and Technology, 18 Hoang Quoc Viet, Hanoi, Vietnam

²Department of Physics and Technology, Thai Nguyen University of Sciences, Vietnam

³Vinh University, 182 Le Duan, Vinh, Vietnam

⁴Institute for Tropical Technology, Vietnam Academy of Science and Technology, 18 Hoang Quoc Viet Road, Hanoi, Vietnam

*Email: oanhvtk@ims.vast.ac.vn

Abstract. The thermal decomposition method is often used to synthesize nanoparticles due to this method can prepared monodisperse nanoparticles with uniformed size. Especially, this method may be controllable size and shape by varying the temperature, precursor concentration and surfactant concentration ratio. In this paper, we investigate synthesis of Fe₃O₄ nanoparticles of different size and shapes by thermal decomposition method. The standard phase of the spinel structure of Fe₃O₄ on XRD patterns confirmed the formation of Fe₃O₄ nanoparticles. TEM micrographs show that the monodisperse nanoparticles with uniformed size. The saturation magnetization as high as 78 emu/g along with the average particle size of 15 nm was obtained from Fe₃O₄ nanoparticles synthesized at 298 °C in 2 hours. The effect of size and shape on characteristics of Fe₃O₄ nanoparticles will be presented and discussed in details.

Keywords: Fe₃O₄ nanoparticles, Saturation magnetization, Shape anisotropy, Thermal decomposition method

1. Introduction

In recent years, magnetic nanoparticles (MNPs) have been of considerable scientific interest of national and international scientists thanks to their abilities to be applied in many fields of science such as: biomedicine, catalysis [1] and magnetic data storage [2]. In biomedical field, requirement of capacity to control morphology, monodispersed and chemical composition of MNPs holds an important role due to the fact that both physical and chemical properties of the MNPs strongly depend on these factors. Recently, various approaches have been employed to synthesize MNPs with different sizes and shapes, for example: co-precipitation, hydrothermal, solvothermal, electro-chemical, reverse micelle and synthesis in organic solvent (thermal decomposition) [3,4]. Among these approaches, synthesis in organic solvent is considered as the best method for MNPs production, especially Fe₃O₄ MNPs, which attract a lot of interests due to their specific properties and potential applications in biomedicine [5,6]. Fe₃O₄ MNPs can be applied in targeting drug delivery, hyperthermia and contrast enhancement of magnetic resonance imaging (MRI) owing to their high saturation magnetization, low cytotoxicity and biocompatibility [7,8].

Until now, successes in controlling size and shape of Fe₃O₄ MNPs have been efficiently reached only with thermal decomposition method by using a large amount of toxic and expensive precursors. For example, iron pentacarbonyl [Fe(CO)₅] was employed to synthesize monodispersed γ -Fe₂O₃ MNPs with average size of 4 -16 nm by adjusting molar ratio of precursors and concentration of surfactant [9]. Sun et al. prepared Fe₃O₄ MNPs using an organic salt, Fe(acac)₃, as precursor and hexadecanediol (HDD) as a reductant. The advantage of this approach was its ability to synthesize MNPs at as high quality as using [Fe(CO)₅]. However, HDD is very expensive and there are still inconsistent opinions about its role in synthesis of MNPs [10].

In this paper, we present our method to synthesize Fe₃O₄ MNPs by thermal decomposition approach without toxic precursors and expensive reductant. Acetylacetonate Fe(acac)₃ and Oleylamine were employed to overcome the drawbacks indicated above. By adjusting precursor concentration and concentration ratio between surfactant oleic acid (OA) and oleylamine (OLA), we could obtain NPs with different size and shape. Structure, morphology and magnetic properties of our samples were carried out, analyzed, compared and discussed in detail.

2. Experimental details

2.1. Chemicals

Iron (III) acetylacetonate (Fe(acac)₃), oleylamine (OLA) and oleic acid (OA) purchased from Sigma-Aldrich.

2.2. Synthesis of Fe₃O₄ nanoparticles

The chemical reagents including Fe(acac)₃, oleic acid (OA) and oleylamine (OLA) were placed into a reaction flask containing 40 ml dibenzyl ether. The mixture was continuously stirred during 30 minutes before being heated to different reaction temperatures for different reaction times. Heating rate was set at 5 °C/min for 25 – 100 °C period, at 7 °C/min for 100 – 200 °C period and at 7 °C/min for 200 – 298 °C period. After reaction, the mixture was naturally cooled down to room temperature and then the particles were washed with ethanol in support of centrifugation before being dispersed in n-hexane.

Samples with different particle sizes were prepared at different concentration of precursor Fe(acac)₃ of 2 mM, 4 mM, 6 mM and 8 mM while the other factors were kept constant: concentration of surfactant OA/OLA of 168 mM, reaction temperature of 298 °C, reaction time of 2h, and were labeled as S1, S2, S3 and S4, respectively.

Samples with different particle shapes were prepared at different concentration of surfactant OA/OLA of 168 mM and OA/OLA of 336 mM while the other factors were kept constant: concentration of precursor of 6 mM, reaction temperature of 298 °C, reaction time of 2h, and were labeled as S5 and S6, respectively.

2.3. Characterization of Fe₃O₄ nanoparticles

The crystal structures of the samples were characterized by using diffractometer SIEMENS D5000 with Cu-K α radiation ($\lambda = 1.5406 \text{ \AA}$) at room temperature. Morphology (size and shape) of the particles were obtained by transmission electron microscopy TEM (JEM 1010). The saturation magnetization of the samples at room temperature was measured under the highest magnetic field of 10 kOe using a vibrating sample magnetometer (VSM) (home-made).

3. Results and discussion

3.1. Effect of precursor concentration on properties of Fe₃O₄ MNPs

In general, the formation and development of MNPs in thermal decomposition approach depend on temperature and reaction time. Besides, concentration of precursors also plays an important role. Some authors indicated that if the precursor concentration is not compatible with volume of solvent in reaction mixture (including surfactants and reaction solvent), it is difficult to control particles size [11-13]. Therefore, in this work, influence of precursor concentration on properties of MNPs was studied to obtain particles at various size ranges. The samples were labeled as S1, S2, S3 and S4 corresponding to concentration of precursor of 2, 4, 6 and 8 mM. Reaction time was fixed at 2 h and reaction temperature was kept at 298 °C (boiling temperature of dibenzyl ether). Morphology, size and

shape of the particles were analyzed through transmission electron microscopy images (TEM) presented in Fig. 1.

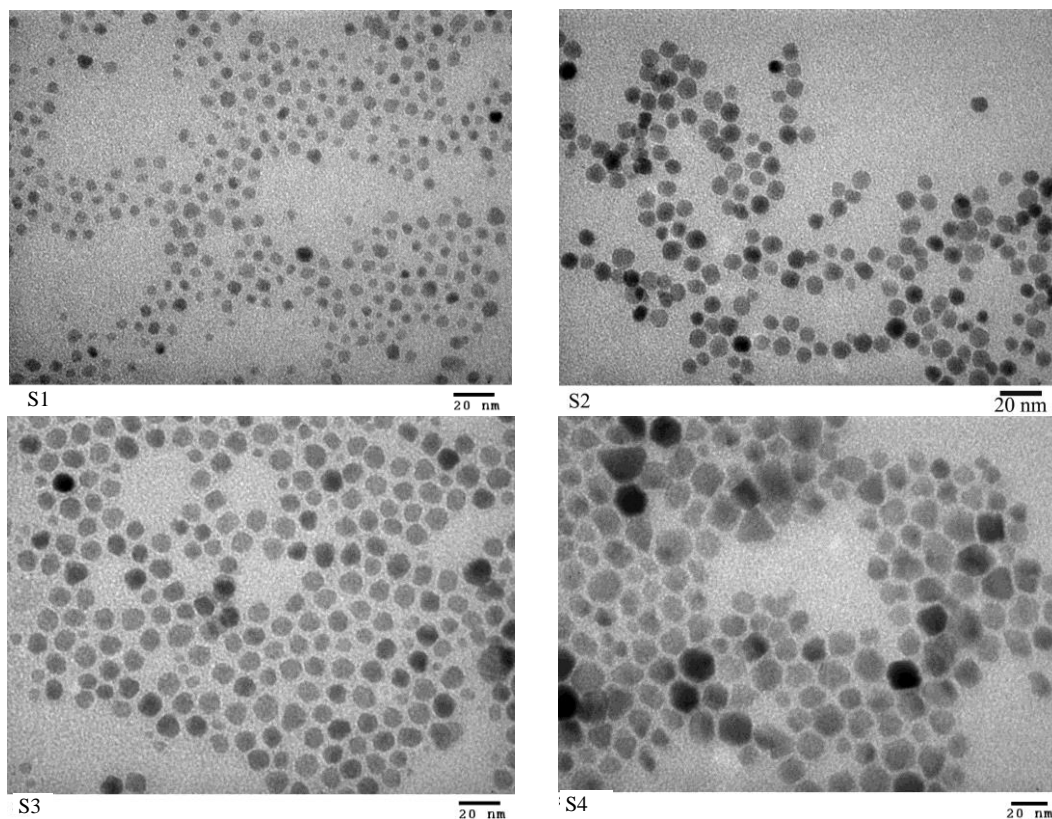


Figure 1. TEM images of Fe_3O_4 MNPs samples synthesized at different concentration of precursor in 2 h of reaction time at 298 °C.

Fig. 1 shows TEM images of Fe_3O_4 MNPs samples synthesized at different concentration of precursor. We can see that all samples contain spherical NPs with relatively homogenous size. After analyzing size distribution of NPs, we found that when increased precursor concentration, particle sizes increased as following: average size increased from 5.5 nm, 8.5 nm, 14.7 nm and 19.6 nm corresponding to sample S1, S2, S3 and S4. In detail, in sample S1 which was of the lowest concentration of precursor, particles had smallest average size of about 5.5 nm, homogenous distribution and clear particle boundary. When precursor concentration was raised to 4 mM (sample S2) and 6 mM (sample S3), average size grew up to about 8.5 nm and 14.7 nm, respectively, particles distributed homogenously and particles boundary was clearer than those of sample S1. Moreover, at higher $\text{Fe}(\text{acac})_3$ concentration of 8 mM (sample S4), particle sizes kept increasing up to about 19.6 nm in average. However, particles dispersion was less homogenous and seemed to aggregate. This trend suggests that at high concentration of precursor small particles incorporate together to form bigger particles. This phenomenon called Ostwald ripening was explained by some groups during the time [12,13]. Magnetic properties of these samples were also determined by measuring $M(H)$ and presented in Fig. 2.

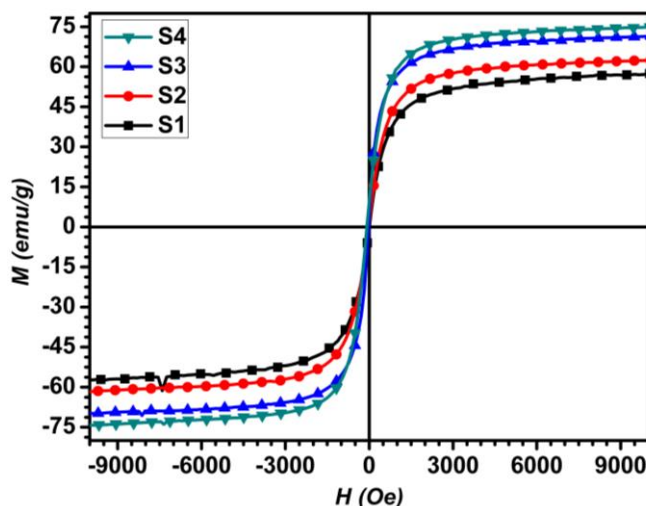


Figure 2. $M(H)$ curves of Fe_3O_4 samples at different concentration of precursor in 2 h of reaction time at $298^\circ C$.

As shown in Fig. 2, when precursor concentration increased, magnetization of samples increased (detail in Table 1). This is a result of increasing particles size caused by higher concentration of precursor, and therefore magnetization increased, as explained by other authors [14-16].

Table 1. Average particle diameter (D_{TEM}), saturation magnetization at 10 kOe (M_{10kOe}) of Fe_3O_4 samples at different concentration of precursor.

Sample	S1	S2	S3	S4
Precursor concentration (mM)	2	4	6	8
D_{TEM} (nm)	5.5 ± 0.5	8.5 ± 0.8	14.7 ± 1.0	19.6 ± 1.5
M_{10kOe} (emu/g)	54	62	71	75

We can easily see in Table 1 that at the lowest concentration of $Fe(acac)_3$ of 2 mM, sample S1 had a low M_{10kOe} value of only 54 emu/g when that of sample S2, which was synthesized at higher concentration of $Fe(acac)_3$ of 4 mM, significantly grew up to 62 emu/g. Saturation magnetization at 10 kOe expressively improved and reached 71 emu/g and 75 emu/g when precursor concentration was used at 6 mM and 8 mM. Although sample S4 had higher magnetization but its particles were bigger and more heterogeneous distribution compared to sample S1, S2 and S3. In fact, our objective is to synthesize MNPs at different size ranges to determine their magnetic properties and aim to apply the sample in biomedicine. Sample S3 is the most suitable to biomedical applications and therefore the precursor was not studied at higher concentration.

3.2. Effect of surfactant concentration on magnetic properties of Fe_3O_4 MNPs

Beside size, shape of MNPs is also an important factor that affects their physical and chemical properties. In this section, we fabricated cube MNPs with asymmetrical in addition to spherical MNPs to compare their properties. Effect of shape on structure is presented in Fig. 3.

In Fig. 3, it can be found that X-ray diffraction (XRD) patterns of all samples contain particular peaks of ferit spinel structure at (220), (311), (400), (442), (511) and (440). Beside specific peaks which are representative for spinel crystal structure of oxides, there was no strange peak, in other words, all the samples were monophasic. Specially, in XRD of cube NPs (S6) there was a new peak appeared (222). We assume that cubic structure enhances crystallization and crystal size of material [17,18]. Crystallite size of MNPs was also qualitatively examined through the width of the peaks shown in Fig. 3. Overallly, peak widths of both the two samples were similar indicated that there was

insignificant change of particle size when it varied from spherical to cubic structure. To further determine size and real shape of MNPs, TEM images of samples were collected and presented in Fig. 4.

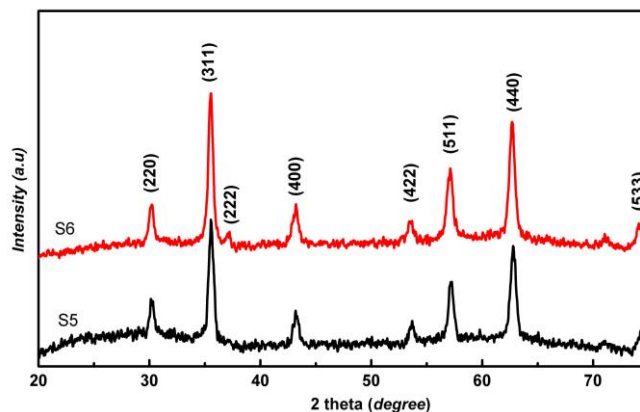


Figure 3. X-ray pattern of Fe_3O_4 powdered samples with spherical NPs (S5) and cube NPs (S6).

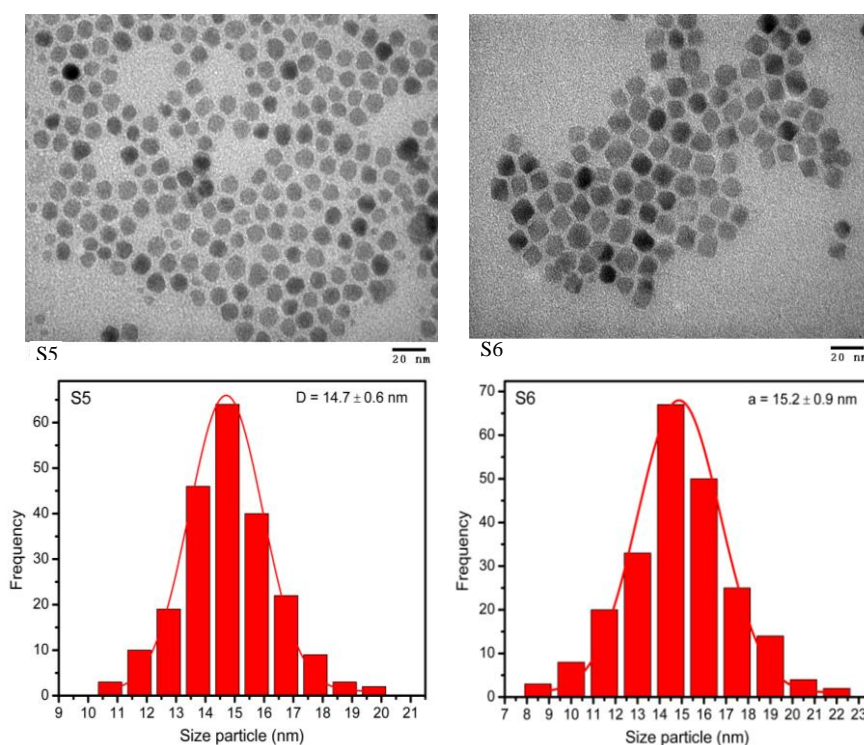


Figure 4. TEM images and size distribution diagram of Fe_3O_4 samples with spherical NPs (S5), cube NPs (S6).

From Fig. 4, we found that in the same reaction conditions, increasing surfactant concentration results in cube NPs. This kind of particles had well-defined boundary compared to that of spherical particles. This result points out that cubic structure leads to better crystallization than spherical one. As indicated in size distribution diagram, particle size of these two samples were irrelevant different. This observation is consistent with what was indicated from peak width in XRD in Fig. 3. Variation of magnetic property of samples with different particle shape was determined through measuring M (H) and shown in Fig. 5.

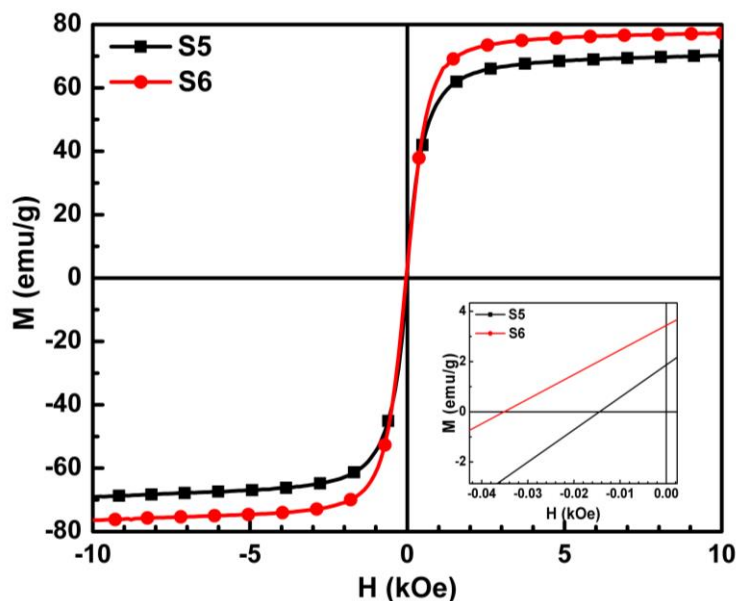


Figure 5. $M(H)$ curves of Fe_3O_4 samples with spherical NPs (S5) and cube NPs (S6).

Fig. 5 shows that the saturation magnetization of cube NPs is higher than that of spherical one. Coercivity (H_c) of cube NPs (S6) is 2.4 times higher than that of spherical NPs (S5). This is a result of shape anisotropy. The saturation magnetization M_s of cube NPs is also consistent with results of XRD (Fig. 3) and of TEM images (Fig. 4). The average particle diameter (D_{TEM}), M_s and H_c were listed in Table 2.

Table 2. Average particle sizes (D_{TEM}), saturation magnetization (M_s) and coercivity (H_c).

	D_{TEM} (nm)	M_s (emu/g)	H_c (Oe)
S5	14.7 ± 0.6	71.2	14.6
S6	15.2 ± 0.9	78.1	35.3

4. Conclusion

Fe_3O_4 MNPs were successfully fabricated at different size ranges through investigating the effect of precursor concentration. Particle sizes grew from 5.5 nm to 19.6 nm corresponding to the precursor concentration increased from 2 mM to 8 mM. About effect of particle shape, two kinds of particles taken into consideration were symmetrical (spherical) and asymmetrical (cube) shape. Results showed that cube NPs had higher crystallization expressed as its maximum saturation magnetization of 78 emu/g. Cube NPs with high saturation magnetization and uniform size could be a good candidate for biomedical application, especially hyperthermia and MRI contrast enhancement.

Acknowledgments

This research is funded by Vietnam National Foundation for Science and Technology Development (NAFOSTED) under grant number 103.02-2017.339.

References

- [1] Qian X, Qin H, Meng T, Lin Y, Ma Z 2014 *Materials* **7** 8105.
- [2] Markovich G 2001 *Amer. Chem. Soc.* **123** 12798.
- [3] Daou T J, Pourroy G, Bégin-Colin S, Grenèche J M, Ulhaq-Bouillet C, Legaré P, Bernhardt P, Leuvrey C, Rogez G 2006 *Chem. Mater.* **18** 4399.

- [4] Hariani P L, Faizal M, Ridwan, Marsi, Setiabudidaya D 2013 *International Journal of Environmental Science and Development* **4** 336.
- [5] Lee J-H, Huh Y-M, Jun Y-w, Seo J-w, Jang J-t, Song H-T, Kim S, Cho E-J, Yoon H-G, Suh J-S, Cheon J 2007 *Nat. Med.* **13** 95.
- [6] Seo W S, Lee J H, Sun X, Suzuki Y, Davidmann, Liu Z, Terashima M, Yang P, Mcconnell M V, Nishimura D G, Dai H 2006 *Nature Mater.* **5** 971.
- [7] Sun S, Zeng H, Robinson D B, Raoux S, Rice P M, Wang S X, Li G 2004 *J. Am. Chem. Soc.* **126** 273.
- [8] Maity D, Choo S-G, Yi J, Ding J, Xue J M 2009 *J. Magn. Magn. Mater.* **321** 1256.
- [9] Park J, Lee E, Hwang N M, Kang M, Kim S C, Hwang Y, Park J G, Noh H J, Kim J Y, Park J H, Hyeon T 2005 *Angew. Chem. Int. Ed. Engl.* **44** 2873.
- [10] Sun S, Zeng H 2002 *J. Am. Chem. Soc.* **124** 8204.
- [11] Hao R, Xing R, Xu Z, Hou Y, Gao S, Sun S 2010 *Adv. Mater.* **22** 2729.
- [12] Chin S F, Pang S C, Tan C H 2011 *Journal of Materials and Environmental Science* **2** 299.
- [13] Vreeland E C, Watt J, Schober G B, Hance B G, Austin M J, Price A D, Fellows Benjamin D, Monson T C, Hudak N S, Maldonado-Camargo L, Bohorquez A C, Rinaldi C, Huber D L 2015 *Chem. Mater.* **27** 6059.
- [14] Yan A, Liu X, Qiu G, Wu H, Yi R, Zhang N, Xu J 2008 *J. Alloys Compd.* **458** 487.
- [15] Wang J, Sun J, Sun Q, Chen Q 2003 *Mater. Res. Bull.* **38** 1113.
- [16] Faraji M, Yamini Y, Rezaee M 2010 *J. Iran. Chem. Soc.* **7** 1.